Physica B 435 (2014) 163–167

Contents lists available at ScienceDirect

Physica B

journal homepage: www.elsevier.com/locate/physb

Micromagnetic and magneto-transport simulations of nanodevices based on MgO tunnel junctions for memory and sensing applications

Z. Hou [a], A.V. Silva [a,b], D.C. Leitao [a,*], R. Ferreira [c], S. Cardoso [a,b], P.P. Freitas [a,b]

[a] INESC-MN and IN, Rua Alves Redol 9, 1000-029 Lisboa, Portugal
[b] Instituto Superior Tecnico (IST), Av. Rovisco Pais, 1000-029 Lisboa, Portugal
[c] International Iberian Nanotechnology Laboratory (INL), Av. Mestre Jose Veiga, 4715-31 Braga, Portugal

ARTICLE INFO

Available online 27 September 2013

Keywords:
Magnetic tunnel junction
Micromagnetic simulations
Magneto-transport

ABSTRACT

This work provides a systematic simulation study of magnetic tunnel junction (MTJ) nanodevices behavior, consisting of a multilayered stack incorporating an in-plane CoFeB free layer and a synthetic antiferromagnetic CoFe-based pinned layer, and including exchange and interlayer couplings. A finite element tool is used to simulate both the magnetic and magneto-transport behaviors of these MTJ nanopillars with distinct geometries, namely circles with diameter ranging from 20 nm up to 250 nm and ellipses with aspect ratios of 1/2, 1/3 and 1/5, corresponding to sizes from $20 \times 40\ nm^2$ up to $50 \times 250\ nm^2$. This study envisages two clear applications for nanopillars: memory and sensor devices. We address the impact of the nanopillar size on the coercivity and saturation field, as figures of merit for device performance. In particular a competitive sensitivity of 0.15%/Oe is envisaged for sensors with a size of $50 \times 100\ nm^2$. Our results provide a validation of this simulation method as a expedite tool to assist the nanofabrication process.

1. Introduction

Intense research regarding the development of magnetic tunnel junctions (MTJs) has been mainly driven by the magnetic data storage industry [1]. Nowadays sub-micrometric MTJ structures are developed for magnetic random access memories, microwave oscillators [2] and sensors [3]. In particular, attention has been given to MTJs devices with a crystalline MgO barrier, showing up to 604% tunnel magnetoresistance (TMR) at room temperature [4], tunable switching fields and device resistance which increase the output power emitted from spin transfer torque nanooscillators (STNOs) [2] and enhance the sensitivity of sensors [1]. Most works concerning analytical calculations or micromagnetic simulations focus on thick ($\sim$10 nm) single ferromagnetic layers [5] or trilayers [6], usually overlooking the effect of interactions. Only recently, more complex stacks, including synthetic antiferromagnetic (SAF) pinned layers [7] and synthetic ferrimagnetic free layers [8], are being considered in simulation models. Furthermore, and although several experimental reports can be found on the magnetic, magneto-transport and current switching behaviors of CoFeB/MgO MTJs [9,10], simulation studies are still lacking. These can be a straightforward tool to provide deeper insight into the overall device response, therefore yielding design rules over the nanofabrication process [11].

In this work we perform a systematic simulation study on the influence of the nanopillar geometry and size on the device magnetic and magneto-transport behaviors. We consider a complex stack with in-plane free-layer, SAF pinned-layer, and incorporate exchange, oscillatory antiferromagnetic interlayer and ferromagnetic Neel couplings, thus approximating our simulation case to a practical nanofabricated device.

2. Simulation details

Simulations of the magnetic and magneto-transport behaviors were performed using the commercial software SpinFlow3D. This is a finite element simulation tool for coupled spin transport and magnetization processes, where the magnetic behavior is modeled by the time independent solution of the Landau–Lifshitz–Gilbert equation at $T=0$ K [12]. The evolution of the system toward a static equilibrium is achieved by forcing an overdamped dynamical regime, to quickly relax the solution with minimal oscillations.

The studied structure consists of a bottom-lead/seed-layer/antiferromagnet (AFM)/ferromagnetic pinned-layer (PL)/spacer/ferromagnetic reference-layer (RL)/barrier/ferromagnetic free-layer (FL)/cap-layer/top-lead (Fig. 1(a)). The structure corresponds to the stack deposited in a Timaris sputtering tool as described in Fig. 1(a) [9,10,13]. The following input parameters were considered [13]:

* Corresponding author. INESC-MN and IN, Tel.: +351 213100237; fax: +351 21314584.
E-mail address: dleitao@inesc-mn.pt (D.C. Leitao).

0921-4526/$ - see front matter © 2013 Elsevier B.V. All rights reserved.
http://dx.doi.org/10.1016/j.physb.2013.09.039

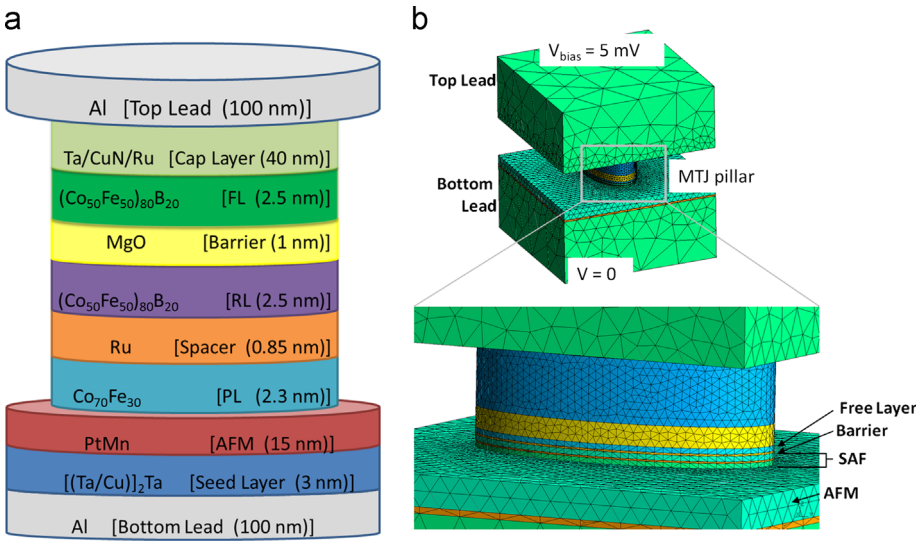

Fig. 1. (a) Schematics of the simulated MTJ pillar with thickness of each layer and corresponding experimental stack. (b) Geometrical model as introduced into the simulation software, with a detail regarding the mesh in each layer.

saturation magnetization (M_s) of 1140 emu/cm^3 and exchange length (l_{ex}) of 3.5 nm for the FL and RL, and M_s=1070 emu/cm^3 and l_{ex}=3 nm for the PL. A uniaxial magnetic anisotropy (H_k) of 15 Oe was considered for the magnetic layers, consistent with the induced anisotropy during film growth. Also, an antiferromagnetic interlayer coupling strength of $J_{SAF}=-0.53$ erg/cm^2 for the SAF, a ferromagnetic coupling of $J_{ferro}=0.02$ erg/cm^2 between FL and RL, and an interfacial exchange coupling strength of $J_{ex}=0.34$ erg/cm^2 between PL and AFM were implemented [13]. For this study we considered either circular pillars with diameter (D) between 20 and 250 nm, and ellipses with aspect ratio (AR=width/length) equal to 1/2, 1/3 and 1/5, corresponding to dimensions varying from (width x length) 20×40 to 50×250 nm^2. All magnetic layers were defined with H_k parallel to the external magnetic field (H_{ext}), ranging linearly from -12 kOe to 12 kOe. The system micromagnetic steady-state configuration was determined for each H_{ext} value. This formulation determines only equilibrium states, not accounting for transient phenomena. The convergence criteria used were $|\vec{u}(t)-\vec{u}(t+dt)|\sim10^{-7}$, on all micromagnetic volumes. To properly define the demagnetizing field (H_d) boundary condition at infinity, the device is enclosed in a spherical shell (~5 times the size of the magnetic sources). The entire device is then discretized using the Frontal unstructured algorithm [14] for both 2D and 3D meshing, resulting in a system of $\sim10^5$ tetrahedral finite elements and $\sim10^4$ triangular vertices (Fig. 1 (b)). The MTJ pillar was meshed with an average element size of 2.5 nm ($<l_{ex}$), while the electrical leads, vacuum and infinity shell were meshed with an element of ~50 nm.

The magneto-transport behavior of the nanopillars in a current perpendicular-to-plane (CPP) geometry was also addressed, using a Valet–Fert formulation for the charge transport in the metallic layers adjacent to the tunnel barrier [15]. Then, a phenomenological non-linear model was used to describe the conductance across the thin barrier, being defined as $g(V_b,\theta)=(g_P(V_b)+g_{AP}(V_b))/2+\cos(\theta)(g_P(V_b)-g_{AP}(V_b))/2$, where g_P (g_{AP}) is the areal conductance in the parallel (antiparallel) configuration, V_{bias} is the bias voltage and θ is the angle between RL and FL magnetization. The second order conductance terms were neglected as small voltage bias (V_{bias}) was considered. Top and bottom leads with $250\times250\times100$ nm^3 and a resistivity (ρ) of 5 μΩcm were placed on either side of the pillar, where a V_{bias}=5 mV was applied (Fig. 1 (b)). Also, $\rho=14$ μΩ cm and a spin diffusion length of 15 nm were considered for the ferromagnetic layers, while $\rho=180$ μΩ cm was used for the AFM layer. Experimentally, nanopatterned structures displayed an average TMR=150% and low $R\times A=5$ Ω μm^2 for the MgO stacks with thin insulator layers (<10 Å) [11,13]. Such values are used as input parameters for simulations by considering g_P=0.2 Ω^{-1} μm^{-2} and g_{AP}=0.08 Ω^{-1} μm^{-2}.

3. Results and discussion

Fig. 2(a) shows the full M (H) behavior for a circular pillar (D=20 nm), with PL (RL) magnetization inversion visible at large negative (positive) fields and FL reversal at low fields. Such a curve mimics the experimental M (H) characterization of a real complex MgO-based MTJ stack [13], with the exception that no PL coercivity was present, as no rotational anisotropy [16], or thermal effects were taken into account. Our studies focus on the FL behavior at moderate applied magnetic fields as befits the envisaged application. Therefore, the inset of Fig. 2(b) depicts the FL M (H) dependence on D: As D increases, M (H) evolved from displaying almost no hysteresis (D=40 nm) to a squared-like curve (D=150 nm). For smaller sizes ($D<120$ nm) a degradation of the memory capability is observed; H_d becomes dominant, resulting in the absence of hysteresis and remanence, consequence of a low H_k. In conclusion, if lower sizes are required for a particular circular device, materials with larger H_k need to be selected for the FL to achieve the desired squared curve. The latter can be experimentally done by tuning the FL material and its thickness at the expense of larger FL coercivity. Fig. 2(b) summarizes the dependence of the coercive (H_c) and offset (H_{off}) fields on D. First, an increase in H_c with D is visible for $D>120$ nm. Such a trend was also observed experimentally [9,13] and is expected if coherent spin rotations were considered [17]. For smaller D, $H_c\sim0$ is observed as discussed above. Fig. 2(b) also depicts H_{off} dependence on D. H_{off} is defined as the deviation of the center of the curve from $H=0$ Oe and includes contributions from the Neel ferromagnetic coupling (~50 Oe for these unpatterned structures [13]) and H_d from the PL. An increase in the absolute value of H_{off} with a decrease in D is observed for $D<120$ nm. This result is consistent with experimental reports [9] with $D<140$ nm, and is probably due to a higher contribution from H_d^{PL}. For $D>120$ nm, an increase